Ellipse Distance Geometry and the Design of 3R Robots

Federico Thomas[1] and Bertold Bongardt[2]

[1] Institut de Robòtica i Informàtica Industrial (CSIC-UPC)
ETSEIB, Diagonal 647, Pavelló E, planta 1, 08028 Barcelona, Spain
[2] Institut für Robotik und Prozessinformatik
Mühlenpfordtstraße 23, 38106 Braunschweig, Germany

Abstract. The study of the power of a point with respect to a circle and its application to orthogonal circles, bundles of circles, etc., has received a lot of attention in the past. In this paper, we show how the concept of conjugate ellipses generalizes the concept of orthogonal circles. It is also shown that it is possible to design 3R serial regional robots whose inverse kinematics can be reduced to the computation of the intersection between two conjugate ellipses which, in turn, can be reduced to the intersection of an ellipse and a line by relying on the concept of radical conic. The relevance of these findings is illustrated through an example.

Keywords: Quartically-solvable robots, quadratically-solvable robots, 3R robots, distance geometry, ellipses.

1 Introduction

Some problems arising in geometry and kinematics can be reduced to computing the intersection of two ellipses. This is the case of, for example, the position analysis of quartically-solvable serial and parallel robots [1], the design of solvable 6R serial robots [2, 3], or the 3P3 problem [4].

Two ellipses intersect in up to four real points which can be obtained as the roots of a quartic polynomial. Nevertheless, as already acknowledged in [2], this algebrization of the problem (using, for example, Chrystal's procedure [5, 6]) complicates the classification and interpretation of degenerate cases. As explained in [7], even when we simply have to compute the roots of a quartic polynomial, it is advantageous to interpret the problem as the intersection of two conics. The superiority of this "geometric approach" has already been exploited to identify cusps and nodes in the singularity locus of 3R serial spatial robots by interpreting their inverse kinematics as the problem of computing the intersection of two ellipses [2, 8].

The geometric approach to the computation of the intersection of two ellipses requires previously classifying their relative position. This operation can be performed by the analysis of the lineal or the exponential pencil defined by both ellipses (see [9, 10] and the references therein). In this paper, we consider only sets of conjugate ellipses; that is, sets of ellipses with parallel axes and the

same eccentricity. We show how the intersection between two such ellipses can be simplified by extending concepts used in the area of Distance Geometry. We then apply these results to identify a family of 3R robots whose quartic closure polynomial simplifies to a quadratic polynomial.

Originally, Distance Geometry was a branch of geometry concerned with characterizing and studying point sets described in terms of point pairwise squared distances, and using the so-called Cayley-Menger determinants to characterize the algebraic dependencies between these distances [11]. Different generalizations of this geometry have led to powerful tools to solve many problems arising in geometry and kinematics. One straightforward generalization has consisted in the incorporation of the relative orientations between simplices. This generalization has permitted obtaining closure polynomials for multiloop linkages, both planar [12] and spatial [13], without relying, in many cases, on variable eliminations. Another generalization has been the substitution of points for spheres. In this case, the distance between points has been substituted with the *power* between spheres, and Cayley-Menger determinants, with the Clifford's identity [14]. In this paper, we go a step further by considering the power of a point with respect to an ellipse, and its application to the characterization of the intersections between conjugate ellipses.

This paper is organized as follows. The power of a point with respect to an ellipse is studied in Section 2. The concept of radical ellipses is introduced in Section 3 where it is applied to the particular case of two conjugate ellipses. The application of this result to the inverse kinematics of 3R robots is presented in Section 4. An example is analyzed in Section 5. Finally, conclusions and prospects for future research are presented in Section 6.

2 The power of a point with respect to an ellipse

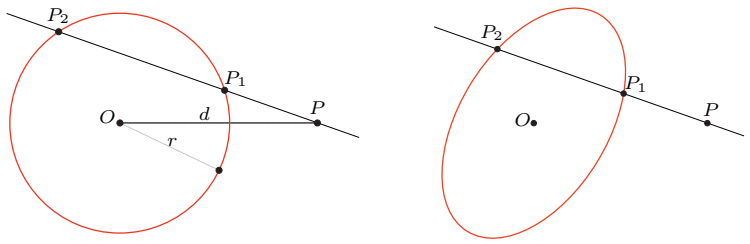

Fig. 1. Left: The power of point P with respect to the circle c is defined as $(c, P) = d^2 - r^2$. It can be proved that $(c, P) = \overrightarrow{PP_1} \cdot \overrightarrow{PP_2}$, independently of the chosen line through P and intersecting the circle. Right: If we likewise try to define the power of a point with respect to an ellipse as $\overrightarrow{PP_1} \cdot \overrightarrow{PP_2}$ the result is not valid as it is not independent of the line.

In 1826, Steiner defined the power of a point P with respect to a circle c of radius r to be $(c, P) = d^2 - r^2$, where d is the distance between P and the center O of the circle [15]. According to this definition, points inside the circle have

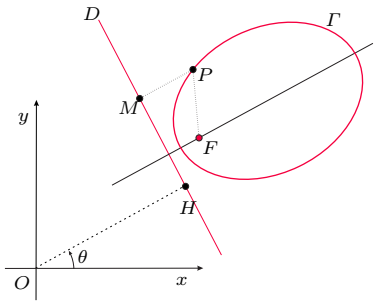

Fig. 2. An ellipse can be characterized as the locus of points P whose distances to point F (one of its two ellipse's foci) and line D (the corresponding directrix) are in a fixed ratio (the ellipse's eccentricity). This property is often taken for a definition of ellipse.

negative power, points outside have positive power, and points on the circle have zero power. Steiner proved that for any line through P intersecting c in points P_1 and P_2, the power of P with respect to c coincides with the inner product $\overrightarrow{PP_1} \cdot \overrightarrow{PP_2}$ (see Fig. 1, left).

In 1865, Laguerre defined the power of a point with respect to an algebraic curve of degree n to be the product of the distances from the point to the intersections of a circle through the point with the curve, divided by the nth power of the diameter d [16]. Laguerre showed that this number is independent of the diameter, but when the algebraic curve is a circle this definition differs from the one given above in a constant factor. This generalization has been revisited at least in [17, 18]. Nevertheless, we prefer a definition for the power of a point with respect to an ellipse from which the above definition of the power of a point with respect to a circle follows as a particular case.

Observe that, if we define $f(x,y) = (x-x_0)^2+(y-y_0)^2-r^2$, then $f(x,y) = 0$ is the implicit equation of a circle centered at (x_0, y_0) and radius r, and $f(x,y)$ is the power of the point, with coordinates (x,y), with respect to this circle. Then, as explained in [17], if $g(x,y) = 0$ is the implicit equation of a conic and we want to attach a geometrical significance to the value of $g(x,y)$ at an arbitrary point of the plane, it is necessary to impose a condition which has the effect of standardizing the function $g(x,y)$ by means of some divisor independent of the variables. Several approaches have been proposed to this end which essentially differ in the chosen parameters defining the ellipse and the chosen divisor [19, 17, 20, 21].

Among all the cited possibilities, the implicit function used by de Biasi in [21] is the one adopted in this paper because the power of a point with respect to a circle derives from it as a limiting case. Moreover, it is embedded with geometric significance which will be fundamental in Section 4 for the analysis of 3D regional robots.

According to Fig 2, let us define the ellipse Γ by one of its foci, say F, and the orthogonal projection of an arbitrary point, say P, onto the associated directrix, say M. Then, the ellipse can be defined as:

$$\Gamma = \{P \mid \overline{PF}^2 - e^2\overline{PM}^2 = 0\}, \tag{1}$$

where e denotes the eccentricity of the ellipse. That is, $e = c/a$ where a is the length of semi-major axis and c is the distance from center to the foci. It is a

measure of how much the ellipse deviates from a circle. It is a number between 0 and 1, with values closer to 0 indicating a more circular shape and values closer to 1 indicating a more ellongated shape.

The power of point P with respect to Γ can be simply defined as

$$(\Gamma, P) = \overline{PF}^2 - e^2\overline{PM}^2. \tag{2}$$

To translate this definition into an algebraic expression in terms of the coordinates of P, let us define $(\alpha, \beta) = \overrightarrow{OF}$ and $h = \overline{OH}$, then the equation of D (see Fig. 2) can be expressed as $x\cos\theta + y\sin\theta - h = 0$, and (2) can be rewritten as

$$\Gamma(x,y) = \begin{pmatrix} x & y & 1 \end{pmatrix} \underbrace{\begin{pmatrix} 1-e^2\cos^2\theta & -e^2\sin\theta\cos\theta & -\alpha+e^2h\cos\theta \\ -e^2\sin\theta\cos\theta & 1-e^2\sin^2\theta & -\beta+e^2h\sin\theta \\ -\alpha+e^2h\cos\theta & -\beta+e^2h\sin\theta & \alpha^2+\beta^2-e^2h^2 \end{pmatrix}}_{\triangleq E} \begin{pmatrix} x \\ y \\ 1 \end{pmatrix}. \tag{3}$$

If δ stands for the 2×2 upper left submatrix of E, it can be verified that $\det(\delta) = 1-e^2$. Thus, the quadratic form in (3) indeed represents an ellipse provided that $1 - e^2 > 0$. It can also be verified that

$$\det(E) = -e^2(\alpha\cos\theta + \beta\sin\theta - h)^2, \tag{4}$$

which is zero for $e = 0$. Apparently, this formulation is not valid for representing circles. The problem is that the eccentricity of a circle is zero and its directrix is the line at infinity. Then, we have to treat circles as limiting cases in which $e \to 0$ and $h \to \infty$. To deal with this circumstance, it is convenient to define $R = eh$ and treat it as an independent variable. Then, E can be rewritten as

$$E = \begin{pmatrix} 1-e^2\cos^2\theta & -e^2\sin\theta\cos\theta & -\alpha+eR\cos\theta \\ -e^2\sin\theta\cos\theta & 1-e^2\sin^2\theta & -\beta+eR\sin\theta \\ -\alpha+eR\cos\theta & -\beta+eR\sin\theta & \alpha^2+\beta^2-R^2 \end{pmatrix}, \tag{5}$$

which, for a circle, reduces to

$$E = \begin{pmatrix} 1 & 0 & -\alpha \\ 0 & 1 & -\beta \\ -\alpha & -\beta & \alpha^2+\beta^2-R^2 \end{pmatrix}, \tag{6}$$

which, when substituted in (3), leads to Steiner's definition of the power of a point with respect to a circle centered at (α, β) and radius R.

The power of a point with respect to an ellipse has many interesting geometric interpretations. Nevertheless, space limitations prevent us from giving more details on this respect. The interested reader is addressed to [20, 21].

3 The radical conic

The set of points of the plane with the same power with respect to two ellipses, say Γ_1 and Γ_2, is the curve defined by $(\Gamma_1, P) = (\Gamma_2, P)$. This is another conic

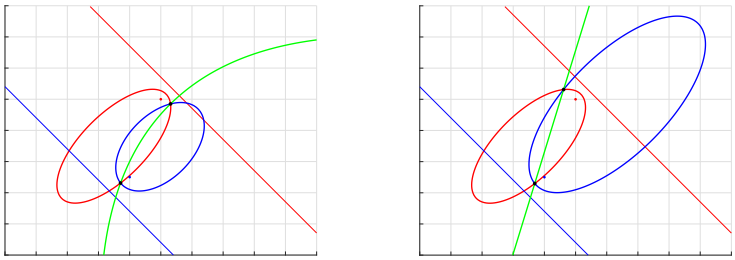

Fig. 3. Configurations of two ellipses in which one of their foci and its associated directrix are depicted in the same color as that of the corresponding ellipse. The radical conic appears in green. The directrices of both ellipses are parallel, but in one case their eccentricities are different (left), and in the other case they coincide (right).

that belongs to the pencil defined by Γ_1 and Γ_2 [20, 21]. As any other element of the pencil, the radical conic contains the intersections of Γ_1 and Γ_2.

Now, let us consider two conjugate ellipses. That is, two ellipses with parallel focal axes (or, parallel directrices) and the same eccentricity. In this case, the entries of the 2×2 upper left submatrix of the matrix defining the radical conic vanish. As a consequence, it can be easily proved that the radical conic degenerates into the line with equation

$$\begin{aligned} 2\left[(\alpha_2{-}\alpha_1) - (h_2{-}h_1)e^2\cos\theta\right]x + 2\left[(\beta_2{-}\beta_1) - (h_2{-}h_1)e^2\sin\theta\right]y \\ + e^2(h_2^2{-}h_1^2) + \alpha_1^2{-}\alpha_2^2 + \beta_1^2{-}\beta_2^2 = 0. \end{aligned} \tag{7}$$

The intersection of this line with either Γ_1 or Γ_2 gives us the points of intersection between Γ_1 or Γ_2. As a clarifying example, consider the two ellipse pairs in Fig. 3. One of its foci and associated directrix are depicted in the same color as that of the corresponding ellipse. On the left hand side, the directrices of both ellipses are parallel, but their eccentricities are different. In this case the radical conic, shown in green, is another ellipse. On the right hand side, when they also have the same eccentricity, the radical conic degenerates into a line (Fig. 3-right). We conclude that two conjugate ellipses can have no more than two intersection points.

4 Application to the design of 3R robots

The analysis of the inverse kinematics of 3R robots using Distance Geometry has been extensively treated in [8, 6]. Next, we summarize the main points of this formulation needed to apply the previous results to the kinematic analysis and design of 3R robots.

Consider the 3R regional robot depicted in Fig. 4, left. Each revolute axis is defined by two points on it. Their exact location along the axes is irrelevant as long as they are far apart to avoid numerical instabilities. Let us denote these points $P_1, \ldots, P_6$, and P_7, the location of the robot's end-effector. Since the distances between the points in two consecutive axes do not depend on the robots'

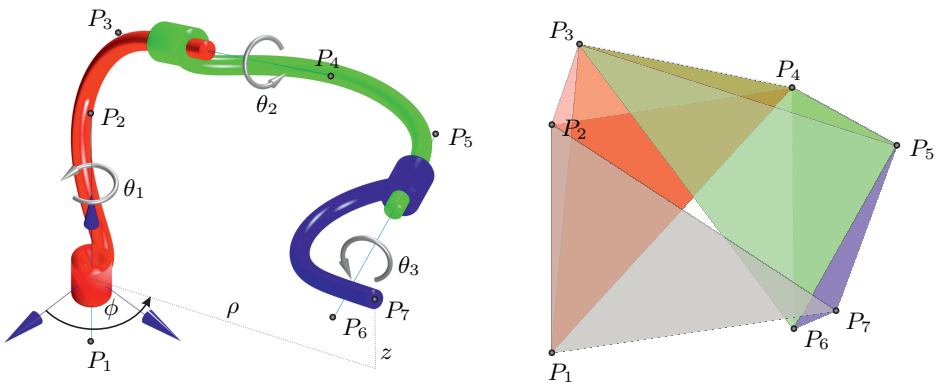

Fig. 4. A general 3R robot (left), and its associated bar-and-joint framework consisting of two tetrahedra –in green and red– and two triangles –in gray and blue– (right).

configurations, we can associate with this robot the bar-and-joint framework appearing in Fig. 4-right. In most distance-based formulation, it is necessary to incorporate in the problem formulation the orientations of the tetrahedra appearing in the corresponding bar-and-joint framework, but this is not necessary in this particular problem [8].

If the z-axis of the world reference frame is aligned with the first revolute joint axis, then it is convenient to express the robot's end-effector location in cylindrical coordinates (ϕ, ρ, z). As a result, the inverse kinematics of this robot boils down to obtaining the rotation angles θ_2 and θ_3 from z and ρ, and trivially obtaining θ_1 from ϕ. Therefore, the inverse kinematics of this robot is essentially equivalent to derive $s_{7,3}$ and $s_{7,4}$ from $s_{1,7}$ and $s_{2,7}$, where $s_{i,j}$ stands for the squared distance between P_i and P_j. To this end, observe that the sets of points $\{P_1, P_2, P_3, P_4, P_7\}$ and $\{P_3, P_4, P_5, P_6, P_7\}$ define a simplex in R^4. Nevertheless, since we are in R^3, their volume is zero. This translates, using the theory of Cayley-Menger determinants, into the following algebraic conditions:

$$\begin{vmatrix} 0 & 1 & 1 & 1 & 1 & 1 \\ 1 & 0 & s_{1,2} & s_{1,3} & s_{1,4} & s_{1,7} \\ 1 & s_{2,1} & 0 & s_{2,3} & s_{2,4} & s_{2,7} \\ 1 & s_{3,1} & s_{3,2} & 0 & s_{3,4} & s_{3,7} \\ 1 & s_{4,1} & s_{4,2} & s_{4,3} & 0 & s_{4,7} \\ 1 & s_{7,1} & s_{7,2} & s_{7,3} & s_{7,4} & 0 \end{vmatrix} = 0 \quad \text{and} \quad \begin{vmatrix} 0 & 1 & 1 & 1 & 1 & 1 \\ 1 & 0 & s_{3,4} & s_{3,5} & s_{3,6} & s_{3,7} \\ 1 & s_{4,3} & 0 & s_{4,5} & s_{4,6} & s_{4,7} \\ 1 & s_{5,3} & s_{5,4} & 0 & s_{5,6} & s_{5,7} \\ 1 & s_{6,3} & s_{6,4} & s_{6,5} & 0 & s_{6,7} \\ 1 & s_{7,3} & s_{7,4} & s_{7,5} & s_{7,6} & 0 \end{vmatrix} = 0. \quad (8)$$

The above two equations are quadratic forms in the unknown distances $s_{3,7}$ and $s_{4,7}$. They actually represent two real ellipses, $\mathcal{A} : z^T A z = 0$ and $\mathcal{B} : z^T B z = 0$, where $z = (s_{3,7}, s_{4,7}, 1)$ and

$$A = \begin{pmatrix} a_1 & c_1 & d_1 \\ c_1 & b_1 & e_1 \\ d_1 & e_1 & f_1 \end{pmatrix} \quad \text{and} \quad B = \begin{pmatrix} a_2 & c_2 & d_2 \\ c_2 & b_2 & e_2 \\ d_2 & e_2 & f_2 \end{pmatrix}. \quad (9)$$

The entries of A and B can, in turn, be expressed as follows:

$$a_1{=}-\begin{vmatrix} 0 & 1 & 1 & 1 \\ 1 & 0 & s_{1,2} & s_{1,4} \\ 1 & s_{1,2} & 0 & s_{2,4} \\ 1 & s_{1,4} & s_{2,4} & 0 \end{vmatrix}, \qquad b_1{=}-\begin{vmatrix} 0 & 1 & 1 & 1 \\ 1 & 0 & s_{1,2} & s_{1,3} \\ 1 & s_{1,2} & 0 & s_{2,3} \\ 1 & s_{1,3} & s_{2,3} & 0 \end{vmatrix}, \qquad c_1{=}\begin{vmatrix} 0 & 1 & 1 & 1 \\ 1 & 0 & s_{1,2} & s_{1,3} \\ 1 & s_{1,2} & 0 & s_{2,3} \\ 1 & s_{1,4} & s_{2,4} & s_{3,4} \end{vmatrix},$$

$$d_1{=}-\begin{vmatrix} 0 & 1 & 1 & 1 & 1 \\ 1 & 0 & s_{1,2} & s_{1,4} & \boxed{s_{1,7}} \\ 1 & s_{1,2} & 0 & s_{2,4} & \boxed{s_{2,7}} \\ 1 & s_{1,4} & s_{2,4} & 0 & 0 \\ 1 & s_{1,3} & s_{2,3} & s_{3,4} & 0 \end{vmatrix}, \; e_1{=}-\begin{vmatrix} 0 & 1 & 1 & 1 & 1 \\ 1 & 0 & s_{1,2} & s_{1,3} & \boxed{s_{1,7}} \\ 1 & s_{1,2} & 0 & s_{2,3} & \boxed{s_{2,7}} \\ 1 & s_{1,3} & s_{2,3} & 0 & 0 \\ 1 & s_{1,4} & s_{2,4} & s_{3,4} & 0 \end{vmatrix}, \; f_1{=}\begin{vmatrix} 0 & 1 & 1 & 1 & 1 & 1 \\ 1 & 0 & s_{1,2} & s_{1,3} & s_{1,4} & \boxed{s_{1,7}} \\ 1 & s_{1,2} & 0 & s_{2,3} & s_{2,4} & \boxed{s_{2,7}} \\ 1 & s_{1,3} & s_{2,3} & 0 & s_{3,4} & 0 \\ 1 & s_{1,4} & s_{2,4} & s_{3,4} & 0 & 0 \\ 1 & \boxed{s_{1,7}} & \boxed{s_{2,7}} & 0 & 0 & 0 \end{vmatrix},$$

$$a_2 = -\begin{vmatrix} 0 & 1 & 1 & 1 \\ 1 & 0 & s_{5,6} & s_{5,4} \\ 1 & s_{5,6} & 0 & s_{6,4} \\ 1 & s_{5,4} & s_{6,4} & 0 \end{vmatrix}, \qquad b_2 = -\begin{vmatrix} 0 & 1 & 1 & 1 \\ 1 & 0 & s_{5,6} & s_{5,3} \\ 1 & s_{5,6} & 0 & s_{6,3} \\ 1 & s_{5,3} & s_{6,3} & 0 \end{vmatrix}, \qquad c_2 = \begin{vmatrix} 0 & 1 & 1 & 1 \\ 1 & 0 & s_{5,6} & s_{5,3} \\ 1 & s_{5,6} & 0 & s_{6,3} \\ 1 & s_{5,4} & s_{6,4} & s_{3,4} \end{vmatrix},$$

$$d_2 = -\begin{vmatrix} 0 & 1 & 1 & 1 & 1 \\ 1 & 0 & s_{5,6} & s_{5,4} & s_{5,7} \\ 1 & s_{5,6} & 0 & s_{6,4} & s_{6,7} \\ 1 & s_{5,4} & s_{6,4} & 0 & 0 \\ 1 & s_{5,3} & s_{6,3} & s_{3,4} & 0 \end{vmatrix}, \; e_2 = -\begin{vmatrix} 0 & 1 & 1 & 1 & 1 \\ 1 & 0 & s_{5,6} & s_{5,3} & s_{5,7} \\ 1 & s_{5,6} & 0 & s_{6,3} & s_{6,7} \\ 1 & s_{5,3} & s_{6,3} & 0 & 0 \\ 1 & s_{5,4} & s_{6,4} & s_{3,4} & 0 \end{vmatrix}, \; f_2 = \begin{vmatrix} 0 & 1 & 1 & 1 & 1 & 1 \\ 1 & 0 & s_{5,6} & s_{5,3} & s_{5,4} & s_{5,7} \\ 1 & s_{5,6} & 0 & s_{6,3} & s_{6,4} & s_{6,7} \\ 1 & s_{5,3} & s_{6,3} & 0 & s_{3,4} & 0 \\ 1 & s_{5,4} & s_{6,4} & s_{3,4} & 0 & 0 \\ 1 & s_{5,7} & s_{6,7} & 0 & 0 & 0 \end{vmatrix}.$$

Since $s_{1,7}$ and $s_{2,7}$ —the boxed entries in the above determinants— depend on the robot pose, only d_1, e_1, and f_1 are variable. This has a very important consequence: the ellipses $\mathcal{A}$ and $\mathcal{B}$ have constant eccentricity and their directrices keep constant orientation, independently of the robot pose.

Without loss of generality, we can assume that $s_{1,2} = s_{5,6}$. If, in addition by design, $s_{1,4} = s_{4,5}$, $s_{2,4} = s_{4,6}$, $s_{1,3} = s_{3,5}$, and $s_{2,3} = s_{3,6}$, then $a_1 = a_2$, $b_1 = b_2$, and $c_2 = c_1$. As a result, the ellipses $\mathcal{A}$ and $\mathcal{B}$ become conjugate: they have the same eccentricity and parallel directrices, independently of the robot pose. Therefore, the maximum number of intersection points between them is two. It can be verified that these constraints make the first and the third revolute axes intersect. The intersection point changes as the second revolute angle varies. This result allows us to identify a family of 3R robots with simple inverse kinematics. A member of this family is analyzed in the next section.

5 Example

According to (8), let us suppose a 3R robot whose associated bar-and-joint framework leads to the following closure algebraic conditions:

$$\begin{vmatrix} 0 & 1 & 1 & 1 & 1 & 1 \\ 1 & 0 & 9 & 13 & 4 & s_{1,7} \\ 1 & 9 & 0 & 31 & 13 & s_{2,7} \\ 1 & 13 & 31 & 0 & 9 & s_{3,7} \\ 1 & 4 & 13 & 9 & 0 & s_{4,7} \\ 1 & s_{1,7} & s_{2,7} & s_{3,7} & s_{4,7} & 0 \end{vmatrix} = 0 \quad \text{and} \quad \begin{vmatrix} 0 & 1 & 1 & 1 & 1 & 1 \\ 1 & 0 & 9 & 13 & 31 & s_{3,7} \\ 1 & 9 & 0 & 4 & 13 & s_{4,7} \\ 1 & 13 & 4 & 0 & 9 & 81 \\ 1 & 31 & 13 & 9 & 0 & 90 \\ 1 & s_{3,7} & s_{4,7} & 81 & 90 & 0 \end{vmatrix} = 0.$$

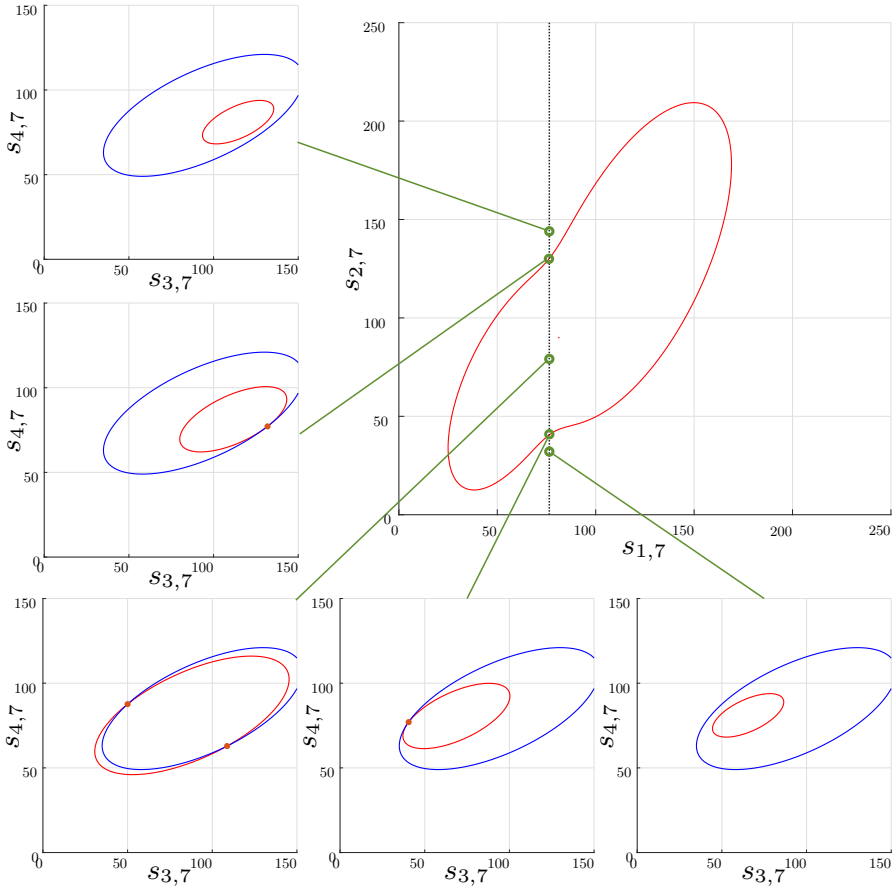

Fig. 5. Singularity locus of the analyzed 3R robot in the distance space defined by $(s_{1,7}, s_{2,7})$. Inside the region determined by this curve locus, there are two solutions for $s_{3,7}$ and $s_{4,7}$, one solution just on it, and none outside the region.

The location of the robot's end-effector determines $s_{1,7}$ and $s_{2,7}$. Once they are set, $s_{3,7}$ and $s_{4,7}$ can be obtained as the intersections of $\mathcal{A}$ and $\mathcal{B}$. In general, two ellipses intersect in up to four points. Nevertheless, since this design satisfies the conditions needed for both ellipses being conjugate, they intersect in no more than two points. Considering that a singularity arises when any two solutions coincide, the singularities of this robot necessarily correspond to those configurations in which both ellipses are tangent (or, equivalently, to those configurations in which the radical line is tangent to any of the two ellipses). This tangency condition leads to the curve shown in Fig. 5, top-right. Each point in this plane defined by $(s_{1,7}, s_{2,7})$ determines a configuration of the two ellipses in the plane defined by $(s_{3,7}, s_{4,7})$. The configurations for five points along the line $s_{1,7} = 79$ are also shown in Fig. 5. The points inside the singularity locus correspond to configurations of the two ellipses intersecting at two points; and outside this region, to non-intersecting ellipses.

We conclude that, while a general 3R is quartically-solvable, the analyzed robot class is quadratically-solvable. Nevertheless, this result comes with a final twist that arises when translating the obtained singularity locus in the distance domain $(s_{1,7}, s_{2,7})$ into the robot's workspace described in cylindrical coordinates (ϕ, ρ, z). To this end, we have to observe that

$$z = \frac{s_{1,2} - s_{2,7} + s_{1,7}}{2\sqrt{s_{1,2}}}, \tag{10}$$

$$\rho = \pm\sqrt{s_{2,7} - (\sqrt{s_{1,2}} - z)^2}. \tag{11}$$

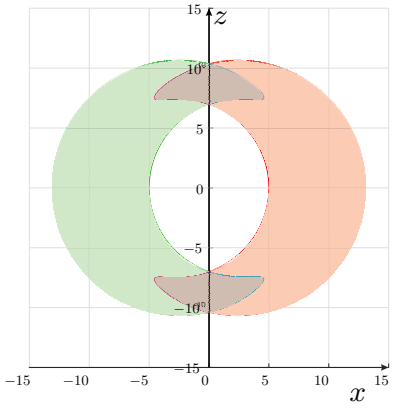

Fig. 6. The result of mapping the singularity locus in Fig. 5 onto the xz cross section of the robot's workspace.

This one-to-two mapping is invariant in ϕ. Due to this invariance, the robot's singularity locus is axisymmetric with respect to the z axis. Fig. 6 presents the outcome of mapping the singularity locus in Fig. 5 onto the xz cross section of the robot's workspace. The resulting plot can be imagined as two overlapping crescent-like shapes. These two symmetric shapes arise due to the duplication resulting from the $\pm$ sign in (11). As a result of this overlapping, all the points of the singularity locus in Fig. 5 are not translated into boundaries of the robot's workspace, some appear as internal singularities and four higher-order singularities show up at $\rho = 0$. Moreover, every point in the overlapping region has four solutions for the inverse kinematics problem despite the analyzed robot is quadratically-solvable.

6 Conclusion

A wrist-partitioned 6R robot consist of a 3R regional robot and a spherical wrist. The 3R regional robot is usually designed so that its inverse kinematics can be simplified to compute the roots of two quadratic polynomials thus leading to up to four solutions. This is accomplished by including orthogonal or parallel consecutive joint axes. We have shown that it is possible to implement 3R regional robots with simple kinematics without relying on this kind of simplifications. The study of the power of a point with respect to an ellipse allowed us to interpret geometrically the symmetric matrix entries associated with the quadratic form defining an ellipse. This, together with the use of a distance-based formulation, has been fundamental to identify this family of 3R robots. We conjecture that other families with equally interesting properties can be identified using the presented approach. Our current efforts concentrate in finding them.

References

1. N. Rojas, J. Borras, and F. Thomas, "On quartically-solvable robots," in *2015 IEEE International Conference on Robotics and Automation (ICRA)*. Seattle, WA, USA: IEEE, 2015, pp. 1410–1415.
2. D. R. Smith, "Design of solvable 6R manipulators," Ph.D. dissertation, Georgia Institute of Technology, 1990.
3. D. R. Smith and H. Lipkin, "A summary of the theory and application of the conics method in robot kinematics," in *Advances in Robot Kinematics*, S. Stifter and J. Lenarčič, Eds. Vienna: Springer, 1991, pp. 81–88.
4. X.-S. Gao, X.-R. Hou, J. Tang, and H.-F. Cheng, "Complete solution classification for the perspective-three-point problem," *IEEE Transactions on Pattern Analysis and Machine Intelligence*, vol. 25, no. 8, 2003.
5. G. Chrystal, *Algebra: An Elementary Text-Book. Part I.* London: A. and C. Black, 1904.
6. F. Thomas and A. Pérez-Gracia, "Some new results in the kinematics of 3R robots using nested determinants," in *ASME 2017 International Design Engineering Technical Conferences and Computers and Information in Engineering Conference (IDETC/CIE 2017)*, Cleveland, Ohio, USA, 2017.
7. W. M. Faucette, "A geometric interpretation of the solution of the general quartic polynomial," *The American Mathematical Monthly*, vol. 103, no. 1, p. 51, Jan 1996.
8. F. Thomas, "A distance geometry approach to the singularity analysis of 3R robots," *ASME Journal of Mechanisms and Robotics*, vol. 8, no. 1, p. 011001, 2015.
9. M. Alberich-Carramiñana, B. Elizalde, and F. Thomas, "New algebraic conditions for the identification of the relative position of two coplanar ellipses," *Computer Aided Geometric Design*, vol. 54, p. 35–48, May 2017.
10. L. Halbeisen and N. Hungerbühler, "The exponential pencil of conics," *Beiträge zur Algebra und Geometrie / Contributions to Algebra and Geometry*, vol. 59, no. 3, p. 549–571, 2018.
11. T. F. Havel, "Some examples of the use of distances as coordinates for Euclidean geometry," *Journal of Symbolic Computation*, 1991.
12. N. Rojas and F. Thomas, "On closed-form solutions to the position analysis of Baranov trusses," *Mechanism and Machine Theory*, vol. 50, p. 179–196, 2012.
13. J. M. Porta and F. Thomas, "Yet another approach to the Gough-Stewart platform forward kinematics," in *2018 IEEE International Conference on Robotics and Automation (ICRA)*, Brisbane, Australia, 2018, pp. 974–980.
14. F. Thomas and J. M. Porta, *Clifford's identity and generalized Cayley-Menger determinants*. Cham: Springer International Publishing, 2021, vol. 15, p. 285–292.
15. J. Steiner, "Einige geometrische Betrachtungen," *Journal für die reine und angewandte Mathematik*, vol. 1, pp. 161–184, 1826.
16. E. N. Laguerre, "Théorèmes généraux sur les courbes planes algébriques," *Comptes Rendus Hebdomadaires des Séances de l'Académie des Sciences*, vol. 60, no. 2, pp. 70–74, 1865.
17. E. H. Neville, "The power of a point for a curve," *The Mathematical Gazette*, vol. 40, no. 331, pp. 11–14, Feb 1956.
18. B. D. Suceavă, A. Vajiac, and M. B. Vajiac, "The power of a point for some real algebraic curves," *The Mathematical Gazette*, vol. 92, no. 523, pp. 22–28, 2008.
19. A. C. Dixon, "Power of a point with respect to a conic," *The Mathematical Gazette*, vol. 6, no. 96, p. 223–223, Jan 1912.

20. A. Loeffler, "Sur la puissance d'un point par rapport à un conique," *Elemente der Mathematik*, vol. 18, pp. 25–28, 1963.
21. J. de Biasi, "Puissance d'un point par rapport à une conique," *Bulletin de l'APMEP (Association des Professeurs de Mathématiques de l'Enseignement Public)*, no. 388, pp. 169–183, 1993.